Predicting Soil Hydraulic Properties for Binary Mixtures - Concept and Application for Constructed Technosols

Moreen Willaredt[1], Thomas Nehls[2], and Andre Peters[1]

[1]Department of Ecohydrology & Landscape Evaluation, Institute of Ecology, Technische Universität Berlin, Ernst-Reuter-Platz 1, 10587 Berlin
[2]Department for Soil Science and Soil Physics, Institute of Geoecology, Technische Universität Braunschweig, Langer Kamp 19c, 38106 Braunschweig

Correspondence: Moreen Willaredt (moreenwillaredt@posteo.de)

Abstract. Constructed Technosols are an important means of substituting natural soil material such as peat and geogenic material for use in urban green infrastructure. One characteristic of Technosols important to their role in urban green infrastructure, specifically in regard to urban water management, are the soil hydraulic properties (SHPs). The SHPs depend on the composition of the constructed Technosols e.g. their components and their mixing ratio. The diversity of possible components and the infinite number of mixing ratios practically prohibit the experimental identification of the composition needed for achieving suitable soil hydrological functions. In this study we propose a compositional model for predicting the water retention curves (WRCs) of any binary mixture based on the measured WRCs of it's two pure components only (basic scheme) or with one additional mixture (extended scheme). The unsaturated hydraulic conductivity curves (HCCs) are predicted based on the modelled WRCs. The compositional model is developed from existing methods for estimating the porosity of binary mixtures. The model was tested on four data sets of measured WRCs of different binary mixtures. The distribution of water and air in $50\,\mathrm{cm}$ high soil columns filled with these mixtures was predicted under hydrostatic conditions in order to assess their suitability for typical urban applications. The difference between the maxima of the pore size distributions $\Delta\mathrm{PSD}_{\mathrm{max}}$ [m] of the components indicates the applicability of the compositional approach. For binary mixtures with small $\Delta\mathrm{PSD}_{\mathrm{max}}$, the water content deviations between the predicted and the measured WRCs range from 0.004 to $0.039\,\mathrm{m}^3\,\mathrm{m}^{-3}$. For mixtures with a large $\Delta\mathrm{PSD}_{\mathrm{max}}$, the compositional model is not applicable. The prediction of the soil hydraulic properties of any mixing ratio facilitates the simulation of flow and transport processes in constructed Technosols before they are produced e.g. for specific urban water management purposes.

1 Introduction

Soil sealing disrupts the natural soil functions involved in regulating water cycles and the energy balance in urban environments. Therefore, environmental problems like pluvial flooding or the intensification of the urban heat island effect are challenging the health and quality of life in urban areas. Climate change intensifies these urgent problems. In fact, plants and their substrates, in the form of green roofs (Molineux et al., 2009; Eksi et al., 2020), facade greening, urban trees pits (Vidal-Beaudet et al., 2018; Yilmaz et al., 2018) and ornamental raised beds (Pitton et al., 2022) can increase the cities' resilience towards extreme

weather events when they are re-introduced to sealed urban areas. The effectiveness of secondary urban greening (Nehls et al., 2015) is dependent upon its brown infrastructure parts (Pouyat et al., 2010). Constructed Technosols, soil-like substrates or growing media restitute the functions of the former unsealed soils on site. This can be described as functional de-sealing. The implementation of urban green infrastructure (UGI) on top of sealed soils leads to an increased demand for soil, planting substrates and constructed Technosols. These constructed Technosols can be engineered from locally accruing mineral and organic waste. This is considered a sustainable path to meet that increased demand (Prado et al., 2020; Deeb et al., 2020; Fabbri et al., 2021), as it reuses materials that would otherwise be land filled. It also decreases the degradation of fertile natural soil resources and other geogenic materials outside urban areas (Willaredt and Nehls, 2021). Tams et al. (2022) showed in a life cycle analysis, that the use of recycled brick particles instead of expanded clay, reduces the $CO2$ footprint of the substrate layer by $50\,\%$ in an extensive green roof. The composition of waste materials and their processing (Ulrich et al., 2021) are the most important design levers in manipulating the properties according to their application (Rokia et al., 2014; Fields et al., 2018; Willaredt and Nehls, 2021). Most UGI address the re-establishment of soil functions related to the regulation of the water cycles (Grabowski et al., 2022). Rokia et al. (2014) were the first to describe the properties of binary and ternary combinations of Technosol components as functions of their mixing ratio and the waste type used. Using dose-response curves they were able to describe six basic soil properties, which are important for agricultural use: total C, available phosphorus, cation exchange capacity, pH in water, the water content at a pressure head of $h = -100\,\mathrm{cm}$ and the bulk density. They showed that only mixtures containing both waste types, mineral and organic, will feature soil-like agronomic properties. Water retention characteristics, hydraulic conductivity and the distributions of water and air for different hydraulic heads determine the successful application of constructed Technosols in UGI (Al Naddaf et al., 2011; Caron et al., 2015). Measurements in soil-like, but still unknown components and in their combinations require the following of a protocol guaranteeing reproducibility of the mixture formulation and comparability between the mixtures (Hill et al., 2019; Willaredt and Nehls, 2021). The extensive labour involved and the costly equipment required, limits comprehensive measuring of the wide variety of components for Technosol construction and their infinite possible mixing ratios.

Therefore, this study aims to develop a concept that allows predicting the WRCs of binary mixtures based on the measured WRCs of only the pure components. Concepts that approach soils as mixtures can be found in research on the soil physical properties after soil amelioration (Abel et al., 2013; Walczak et al., 2002) and in research on soils containing stones or gravel (Naseri et al., 2019; Zhang et al., 2011). The impact of mixing on soil physical properties, mainly porosity and saturated hydraulic conductivity, were most comprehensively described for mixtures of coarse and fine particles with a pronounced particle size difference (Sakaki and Smits, 2015; Zhang et al., 2011; Clarke, 1979). For the porosity in such mixtures the functional dependence on the composition of the mixture has been described by the concepts „ideal mixing“ and „zero mixing“ (Clarke, 1979):

In „ideally mixed“ binary mixtures two categories can be distinguished depending on their mixing ratio: fine-controlled or coarse-controlled mixtures. In fine-controlled mixtures the fine component of the mixture determines its properties, and the coarse particles - having no inner porosity - reduce the total porosity in the mixture. In coarse-controlled mixtures the fine

particles are located within the pores between coarse particles.

In „zero mixed" binary mixtures, the resulting porosity can be linearly interpolated between the components' porosity.

The effect of the volumetric stone content in fine-controlled mixtures on the resulting porosity, as well as on the water retention curve and unsaturated hydraulic conductivity has been successfully described by scaling approaches e.g. from Bouwer and Rice (1984) and Flint and Childs (1984). With high resolution WRC measurements Naseri et al. (2019) confirm the applicability of scaling approaches for stony soils with volumetric stone contents not bigger than the order of magnitude of 30 vol%, hence fine-controlled mixtures. Sakaki and Smits (2015) measured, in addition to the porosity, the WRCs in mixtures with pronounced particle size difference and found the patterns of „ideal mixing" also reflected in the WRCs. The focus on mixtures with components having distinct particle size differences is a major limitation for the transferability of this prediction concept to Technosols. Technosols are mixtures of practice-oriented components with overlapping particle size and pore size distributions e.g. organic and mineral components that present fine graded particle size distributions instead of distinct particle size differences. Therefore, the particles of these components are less likely to be located within each others pore spaces. Hence, the impact of mixing the components on the resulting water retention curves is more likely to be represented by the „zero mixing" concept introduced above.

The purpose of this study is to develop an approach for predicting water retention curves in binary mixtures of materials which are suitable for Technosol construction. This enables the prediction of soil hydraulic properties of Technosols formulated as binary mixtures in any mixing ratio based on only a few necessary measurements. We therefore: i) formulate and use a simple compositional model approach to predict the water retention curves of binary mixtures that cover a full range of mixing ratios (from 0/100 to 100/0 (vol/vol)) based on the WRCs of the pure components, ii) assess the approach with sets of WRCs of binary mixtures found in the literature, and iii) present the applicability of the compositional model for predicting hydraulic conductivity curves and hydrostatic distribution of water and air using the constructed Technosols as planting substrates in a container.

2 Material & Methods

2.1 Concept of compositional models

In this study the difference between the maxima of the pore size distribution (PSD) of both components ΔPSD_{max} [m] is used as a measure to qualitatively evaluate their similarity. It can be calculated as the difference between the logarithms of the effective radii R_{eff} [m] and r_{eff} [m] at the PSD maxima for the components with larger and smaller components respectively:

$$\Delta PSD_{max} = \log_{10}\left(R_{eff}\right) - \log_{10}\left(r_{eff}\right) \tag{1}$$

Figure 1 visualises schematically the proportions of pore radii present in two components and the resulting pore system arrangement with a large ΔPSD_{max} (Fig. 1 a) and a smaller ΔPSD_{max} (Fig. 1 b).
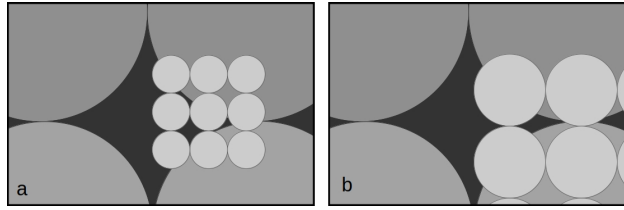
Figure 1. Schematic representation of two pore systems a) presenting a pronounced difference in effective pore radii found in two soil components: The pores of the component characterised by smaller pores can arrange within the pores of the component characterised by large pores („ideal mixing") and b) presenting a smaller difference in pore size radii: The pores formed by the particles in the components characterised by the small pore radius do not easily locate within the larger pore system but rather exist next to each other („zero mixing").
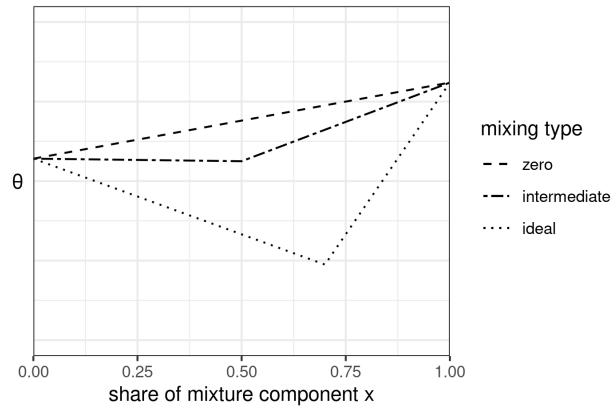
Figure 2. Mixing types of water retention characteristics in binary mixtures (adapted from concept for porosity in binary mixtures in Zhang et al. (2011)).

2.1.1 Adapted Clarke model

The „ideal mixing" approach described in Clarke (1979) was formulated to define the lower boundary of the resulting porosity in binary mixtures of fine and coarse particles. It was developed to describe natural soil containing stones or gravel and distinguishes two cases: „coarse-controlled" mixtures and „fine-controlled" mixtures. The volumetric composition describes the volumetric stone content in the mixture. For fine-controlled mixtures, this implies that the volume of the coarse fraction refers to the solid volume of the contained stones in a background bulk volume of the fine component. The volumetric share of the fine component x_f [-] in the mixture delineates the two cases. The threshold, at which the relation between the porosity and the volumetric share of the fine component changes from one case to the other, corresponds to $x_f = \phi_c$ (Sakaki and Smits, 2015), where ϕ_c [-] stands for the porosity in the coarse component of the binary mixture.

When adapting the „ideal mixing" approach to predict the complete water retention curves for any volumetric composition, we refer to the bulk volumes of the components that form the composition. Hence, x [-] refers to the bulk volumetric share of one component in the mixture (Fig. 2). With the adapted Clarke model the predicted water retention curves are calculated as:

$$\theta_{\mathrm{pred}} = \begin{cases} (\mathrm{x}_f + \phi_c \mathrm{x}_c) \cdot \theta_f, & \text{if } \mathrm{x}_f \geq \phi_{\mathrm{c}}, \\ \left(\phi_c - \frac{\mathrm{x}_f(1-\phi_f)}{\phi_c} \right) \cdot \theta_c + \phi_f \mathrm{x}_f \theta_f, & \text{otherwise} \end{cases} \tag{2}$$

where θ_{pred} [-] is the predicted water retention curve in a mixture and θ_f [-] and θ_c [-] stand for the water retention curves in the fine and coarse components of the mixture respectively. ϕ_f [-] represents the porosity in the fine component, x_f [-] refers to the bulk volumetric share of the fine component and x_c [-] stands for the bulk volumetric share of the coarse component. The volumetric content of fine component is effectively larger in ideally mixed fine-controlled mixtures ($\mathrm{x}_f \geq \phi_{\mathrm{c}}$) compared to the bulk volumetric share of fine particles. The difference corresponds to the porosity in the bulk volumetric share of the coarse component as this volume is filled by fine particles. The volume taken up by the solids of the coarse component does not contribute to water retention. This corresponds to the scaling approaches tested and approved by Naseri et al. (2019). In coarse-controlled mixtures the water retention in the coarse component of the mixture is reduced by the solid volume introduced with the fine component. The water retention within the pores of the fine component adds to the mixtures water retention (Eq. 2). In binary mixtures with pore systems that are characterised by small $\Delta\mathrm{PSD}_{\mathrm{max}}$ [m] the particles and the pore system formed between them are not going to interlock in the same way that mixtures with distinct difference in particle size do. Instead, the particles in the mixture exist next to each other and form a new pore system that can be directly calculated as a linear interpolation between the porosities of the two pure components. In reality, the mixture's porosity and consequently the water retention, likely follows a curves situated between „zero mixing" and „ideal mixing", represented by the „intermediate mixing" type in Fig. 2.

2.1.2 Basic scheme CM1

This approach corresponds to the „zero-mixing" concept and is a weighted superposition of the WRCs of the two components to predict the WRC of the mixture:

$$\theta_{\mathrm{pred}} = \mathrm{x}_{\mathrm{a}} \theta_{\mathrm{a}} + (1 - \mathrm{x}_{\mathrm{a}}) \theta_{\mathrm{b}} \tag{3}$$

where x_{a} [-] and x_{b} [-] represent the bulk volumetric share of component a and b for the mixture, with $\mathrm{x}_{\mathrm{a}} + \mathrm{x}_{\mathrm{b}} = 1$, and where θ_{a} [-] and θ_{b} [-] are the volumetric water contents at any matric potential of the two single components and θ_{pred} [-] is the resulting volumetric water content of the mixture at any matric potential.

2.1.3 Extended scheme CM2

For the extended scheme of the compositional model, an additional WRC is required for predicting a mixture's WRC. The additional WRC should represent a mixture of similar shares of both components. Therefore it is referred to as the WRC of an

Table 1. Properties of components constituting the investigated binary mixtures. Porosity, if not provided, was calculated from particle density, bulk density and soil sample volume.

Property		Willaredt & Nehls 2021		Walczak et al. 2002		Deeb et al. 2016		Sakaki & Smits 2015	
		GB	GWC	S	P	EDH	GWC	CS	FS
BD	$[\mathrm{g\,cm^{-3}}]$	1.35	0.64	1.86	0.33	1.17	0.37	1.77	1.74
PD	$[\mathrm{g\,cm^{-3}}]$	2.63	2.32	NA	NA	2.75	2.06	2.65	2.65
C concentration	$[\mathrm{g\,kg^{-1}}]$	24	268	1	574	0.38	214	NA	NA
porosity	$[\mathrm{m^3\,m^{-3}}]$	0.49	0.69	0.38	0.9	0.57	0.82	0.34	0.34

GB: ground bricks, GWC: green waste compost, P: peat, S: sand, EDH: excavated deep soil horizon, CS: coase sand, FS: fine sand

intermediate mixture x_m [-] (intermediate mixing concept in Fig. 2). The motivation behind the extended scheme is to analyse if a slight increase in measurement effort leads to more sound predictions. With the extended scheme the predicted water retention curves are calculated as:

$$\theta_{\mathrm{pred}} = \begin{cases} \frac{x_a}{x_m}\theta_m + \left(1 - \frac{x_a}{x_m}\right)\theta_b, & \text{if } x_a < x_m, \\ \frac{1-x_a}{1-x_m}\theta_m + \left(1 - \frac{1-x_a}{1-x_m}\right)\theta_a, & \text{if } x_a > x_m, \end{cases} \tag{4}$$

130   where x_m [-] represents the bulk volumetric share of component a in the intermediate mixture and θ_m [-] the water content in the intermediate mixture. This approach is based on typical calculations for dilution concentrations.

2.2   Data sets of binary mixtures and their mathematical representation

2.2.1   Data sets

We used four different data sets of WRCs of binary mixtures, ranging from volumetric shares of the pure first component
135   (100/0) to volumetric shares of the pure second component (0/100) (Tab. 2). Three of them represent binary mixtures of one organic and one mineral component mimicking soils and providing soil functions (Walczak et al., 2002; Deeb et al., 2016; Willaredt and Nehls, 2021). The fourth data set (Sakaki and Smits, 2015) represents a mixture of sands with pronounced difference in particle sizes (Fig. 3). The data of Walczak et al. (2002) was digitally extracted from their graphs using the open access software Engauge-digitizer 12.1 (Mark Mitchell and et al, 2019). The other three data sets were available as raw data.
140   Table 1 summarises selected properties of the components used for composing each of the four data sets.

Deeb et al. (2016) combined excavated deep soil horizon from construction sites (EDH) with green waste compost (GWC) to create mixtures containing GWC shares of 0, 10, 20, 30, 40, 50 and 100 % (vol), denominated C0E10, C1E9, C2E8, C3E7 C4E6, C5E5 and C10E0, respectively. Four replicates of each mixture were put into planting containers. Samples were taken from their surface. The volumetric water contents of the samples were assessed at eight matric potentials h [cm] using the sand

Table 2. Converted volumetric share of peat derived from mass specific mixing ratio and magnitude of resulting error

Sample	$x_{i,v}$ [$cm^3 cm^{-3}$]	$x_{i,m}$ [$g g^{-1}$]	BD_{meas} [$g cm^{-3}$]	BD_{calc} [$g cm^{-3}$]
P0S10	0	0	1.86	1.86
P2S8	0.24	0.5	1.57	1.49
P6S4	0.64	0.2	1.05	0.88
P8S2	0.82	0.4	0.68	0.61
P9S1	0.93	0.6	0.51	0.44
P99S01	0.99	0.8	0.41	0.35
P10S0	1	1	0.33	0.33

145   box method for h of -2, -9.8 and $-31\,cm$ and a pressure-plate apparatus for the matric potentials h of -310, -980, -1550, -4910 and $-15\,540\,cm$.

Walczak et al. (2002) created mixtures of peat and sand with mass specific contents of dry peat $x_{i,m}$ of 0, 0.05, 0.2, 0.4, 0.6, 0.8 and 1 (mass/mass), with i [-] referring to the specific mixture. For our analysis the volumetric peat content $x_{i,v}$ [-] of each mixture was determined based on the given bulk densities (BD_{meas}) and the mass specific contents of the mixtures using

150   the following equation: $x_{i,v} = x_{i,m} \cdot \frac{BD_{meas}}{BD_{peat}}$. The BD of peat and sand are $0.33\,g\,cm^{-3}$ and $1.86\,g\,cm^{-3}$, respectively. Table 2 summarises the volumetric ratios of the mixtures and the deviations between the measured and calculated BD resulting from the conversion of gravimetric to volumetric contents. It indicates the magnitude of error introduced by such a conversion. The sample names of the mixtures reflect the order of magnitude of volumetric peat content. The WRCs of all mixtures were determined by using pressure plate extractors at seven different matric potentials h: -1, -10, -31.6, -100, -158.5, -1000 and

155    $-15\,848.9\,cm$.

Willaredt and Nehls (2021) used different binary mixtures of ground bricks (GB) and green waste compost (GWC) with volumetric shares of GWC of 0, 18, 28, 37, 47, 68, 100 % (volume/volume). The respective denominations refers to the rounded bulk volumetric share of GWC: C0B10, C2B8, C3B7, C4B6, C5B5, C7B3 and C10B0. The water retention curves of five replicates of each mixture were measured combining the simplified evaporation method (Schindler, 1980; Peters et al.,

160   2015), using the HYPROP© device (Metergroup, Munich, Germany) and the dew point method (Campbell et al., 2007) using the WP4C device (Metergroup, Munich, Germany). For details of the measurements and the data evaluation, the reader is referred to Willaredt and Nehls (2021).

Sakaki and Smits (2015) combined coarse sand (mean grain size $D = 1.04\,mm$) and fine sand (mean grain size $d = 0.12\,mm$), thus choosing two components with a pronounced difference in particle size. They obtained water retention measurements with

165   a high resolution for matric potentials ranging between -1 and $-135\,cm$ using an induced drainage process in a modified Tempe cell setup (Sakaki and Illangasekare, 2007).

2.2.2 Mathematical representation

We used the SHIPFIT2.0 software (Peters and Durner, 2015) to fit parametric water retention models to the data. For each data set we chose the model presenting the best performance in regard to matching the observations in the respective measurement range without over parametrisation. The detailed model descriptions and the obtained parameters together with the RMSE between the models and observations are summarised in the Appendix (Tab. A1-A4). The data of Willaredt and Nehls (2021) was measured in high resolution and showed a complex pore structure, thus the PDI model (Peters, 2013; Iden and Durner, 2014; Peters, 2014), with the unconstrained bimodal van Genuchten basic function (van Genuchten, 1980), was fitted to the data (see Eq. A1, A4 and A5). The model was fitted to all replicates of each mixture.

Due to its limited matric potential range but high resolution (Fig. 4), the data sets of Sakaki and Smits (2015) were described with the PDI model using the constrained bimodal van Genuchten function (Durner, 1994) (see Eq. A1, A3 and A5). The data sets of Deeb et al. (2016) and Walczak et al. (2002) have less observations (n=9 and n=7, respectively for each mixture). For those data sets unimodal models were applied, as the fitting of a small number of parameters results in more robust fitting and consequently more robust predictions. The data set by Deeb et al. (2016) was best represented by the PDI model with the unimodal constrained model of van Genuchten (1980) as basic function (see Eq. A1 and A3), whereas the data set of Walczak et al. (2002) was best represented using the original unimodal constrained model of van Genuchten (1980) (see Eq. A3). The latter can be explained by the comparably high remaining water contents at high matric potentials. The fitted curves for the pure components and the intermediate mixtures (referred to as „fit4pred") were used as model input to predict the water retention curves (referred to as „pred") of all binary mixtures. The fitted curves for all other mixtures were used as reference curves (referred to as „fit4ref") to subsequently assess the quality of predictions.

2.3 Testing

We evaluate the predictive performance of the described compositional model approaches by calculating the RMSE between the predicted curves („pred") and the reference curves („fit4ref"):

$$\text{RMSE} = \sqrt{\frac{1}{r} \sum_{i=1}^{r} (\theta_{\text{pred}} - \theta_{\text{fit4ref}})^2}, \tag{5}$$

where θ_{fit4ref} [-] is the water content at the specific matric potential given by the model fitted to the observations, θ_{pred} [-] is the predicted water content using one of the compositional models and r [-] is the number of points on the curves used. We furthermore analyse the absolute deviation as the difference between the predicted and reference water contents at similar matric potentials, meaning that positive deviations indicate that the prediction overestimates and negative deviations underestimate the water contents compared to the value of the reference curve.

2.4 Model application

We demonstrate two ways of applying predicted WRCs for further soil hydrological characterization and selection of suitable Technosol mixtures. For these examples we use the binary mixtures of Willaredt and Nehls (2021) and Deeb et al. (2016) for the use in urban green infrastructure.

2.4.1 Prediction of hydraulic conductivity functions

In order to simulate transport processes in constructed Technosols, not only the WRC but also the unsaturated hydraulic conductivity curve (HCC) is required. However, observations of HCCs, especially in the unsaturated moisture range, are rarely available. Therefore, we used the approaches for absolute non-capillary and capillary conductivity within the PDI scheme outlined by Peters et al. (2021, 2023). Their approach does not require any measured conductivity value as matching point but needs the separation of capillary and non-capillary water retention. The following procedure was applied to achieve this requirement: after predicting the WRCs with our compositional approach outlined above, we re-fitted the same parametric models to the predicted curves. These re-fitted model curves were then used for the prediction of the absolute HCC. In line with Peters et al. (2023), we selected the value of the HCCs at h = $6\,\mathrm{cm}$, corresponding to a pore diameter of $5\,\mathrm{mm}$, to derive the so-called saturated matrix conductivity, $K_{s,matrix}$ $[\mathrm{cm\,d^{-1}}]$, which mimics the saturated conductivity for the case if macro pores are absent.

2.4.2 A case study of predicted water and air distribution

We calculated the distribution of air and water based on the predicted and the reference water retention curves in a containerised constructed Technosol. This demonstrates the application of predicted soil hydraulic properties for a real-world problem. As an example we chose a $0.5\,\mathrm{m}$ high raised bed with constant water saturation at the bottom. We furthermore assume hydrostatic equilibrium and calculate the matric potential across the whole profile, thus the matric potential at the upper boundary is approximately pF 1.7. The air content is simply calculated as $\theta_s - \theta(z)$, where θ_s $[\mathrm{m^3\,m^{-3}}]$ stands for the water content at saturation and $\theta(z)$ $[\mathrm{m^3\,m^{-3}}]$ stands for the water content at the matric potential corresponding to the soil depth z [m] in the container.

3 Results & Discussion

3.1 Pore size distribution in components of binary mixtures

The difference between the maxima of the pore size distributions ΔPSD_{max} [m] of the components provides a useful measure for choosing the right type of model for predicting any mixture's water retention curve. Figure 3 assembles the pore size distribution curves computed for all components used to create binary mixtures. Each plot is supplemented with the value of ΔPSD_{max}. That quantifies the order of magnitude between the size of the most abundantly occurring pore sizes in both components.
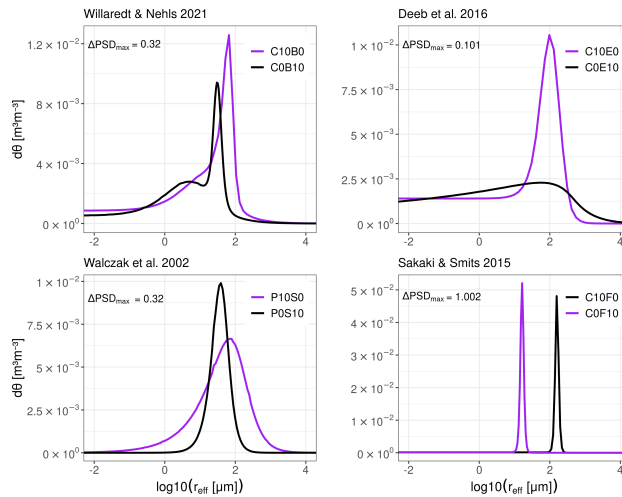
Figure 3. Pore size distribution of each component used to create the binary mixtures. The magnitude of the distance between each curves' maxima ΔPSD_{max} describes the size difference of the most abundantly occurring pores in both components.

In the data of Willaredt and Nehls (2021) the pore size corresponding to the maxima of the PSD in green waste compost (C10B0) is approximately twice as big as the PSD_{max} in ground bricks (C0B10). The sand (P0S10) and peat (P10S0) chosen for the mixtures prepared by Walczak et al. (2002) show a similar difference. The smallest difference was determined for the excavated deep soil (C0E10) and green waste compost (C10E0) (Deeb et al., 2016) with the most abundantly present pores in green waste compost only 1.26 times larger than those on the excavated deep soil horizon. The most pronounced difference between the PSD_{max} was determined for the mixture of coarse sand (C10F0) and fine sand (C0F10) studied by Sakaki and Smits (2015). Here the size difference between the most abundantly occurring pore size in coarse sand is 10 times larger than the dominant pore size found in fine sand. The PSD of the components that are relevant for Technosol construction (i.e. GWC, ground bricks, peat, sand and excavated deep soil horizon material) show small differences between PSD_{max}. Hence, the difference between them is too small and the two pore systems will not interlock as is the case for the fine and coarse sand used by Sakaki and Smits (2015) (compare Fig. 1). Based on these differences the model type can be selected. The predictions for the data sets by Willaredt and Nehls (2021), Walczak et al. (2002) and Deeb et al. (2016) were predicted using the „zero mixing" approach corresponding to the basic scheme of the compositional models. The model type „ideal mixing" was applied to the data by Sakaki and Smits (2015). In mixtures formulated with more then two components, or with components containing coarse particles with inner porosity (e.g. bricks), three maxima would have to be considered. Not every mode in the single component's PSD is necessarily visible in the mixtures because the PSD may intertwine.

3.2 Impact of data quality and resolution

The pore size distributions in Fig. 3 only show bi-modality for the data set of Willaredt and Nehls (2021), this is likely due to the high resolution of the water retention curve. Therefore, a bimodal parametric model was chosen to represent the

water retention curve. The bi-modality is more pronounced for the ground bricks (C0B10). The assumption is that this is due to their inner porosity, that was found for ground brick particles bigger than $0.2\,\mathrm{mm}$ (Nehls et al., 2013). The green waste compost (C10B0) also has a secondary pore system with most pores having the size of approximately $1\,\mathrm{\mu m}$. It is likely that the green waste compost used in the mixtures formulated by Deeb et al. (2016) presents a similar structure, however due to the comparably small number of observations on the curve, such a structure remains undetected. We therefore stress the importance of high-resolution measurements and a wide range of matric potentials on which the presented predictions of water retention curves of the mixtures should be based. The evaporation method implemented in the HYPROP© device accounts for high resolution measurements, however the measurement range here should be extended towards higher matric potentials by complementary measurements, e.g. with the WP4C dew point water potential meter (Flores-Ramírez et al., 2018). Furthermore, we identify the need for systematically measuring the water retention curves of materials that have been identified as suitable components in Technosol construction (e.g. compiled in Rokia et al. (2014)). A comprehensive data base would be helpful for further validating and narrowing down thresholds of $\Delta\mathrm{PSD}_\mathrm{max}$. So far, $\Delta\mathrm{PSD}_\mathrm{max}$ is a qualitative description and a more precise quantification should be done based on more data sets.

3.3 Predicted water retention curves

The plots in Fig. 4-7 illustrate the comparison between the predicted water retention curves and the reference water retention curves. The first panel in each plot shows the curves of the pure components („fit4pred"), used as model input. The curves are presented together with the corresponding RMSE, that quantifies the average deviation between the predictions and the respective reference curves.

The adapted Clarke model is suitable for predicting the water retention in the fine-controlled mixtures created by Sakaki and Smits (2015). This applies to the mixtures C2F8, C5F5 and C7F3. For coarse-controlled mixtures the Clarke model accounts well for the observations in the wet range, this is unsurprising as it was adapted from a model for porosity prediction. Whereas the air entry point in the mixture C9F1 is not impacted by the small volumetric share of fine sand, in the mixture C2F8 the volumetric share of fine sand effect the curve. Neither the Clarke approach, nor the basic or extended compositional model, properly predict the impact of the addition of small amounts of fine sand to the mixture. This can be explained by the heterogeneity of such a mixture which develops when some of the pores formed by the large particles are filled with fine particles whilst others remain empty (Naseri et al., 2019). Mixtures of coarse and fine sand are not relevant for Technosol construction in practice. However, coarse expanded geogenic particles with inner porosity are popular commercial components in green roof media and horticultural substrates (Hill et al., 2019). The description of their water retention characteristics by Flores-Ramírez et al. (2018) show a clear bimodal pore structure. For constructed Technosols, that contain coarse fragments with inner porosity, a modified version of the Clarke model that accounts for water retention within the coarse particles, could be applied.

For the data set of Willaredt and Nehls (2021) the fitting quality of the mathematical representations is characterised by RMSEs ranging between $0.005\,\mathrm{m}^3\,\mathrm{m}^{-3}$ for the mixture C4B6 in the best case and $0.02\,\mathrm{m}^3\,\mathrm{m}^{-3}$ for the mixture C5B5 in the worst case (see Tab. A1 for model specification and all RMSE). The averaged deviation between the predicted WRC and the
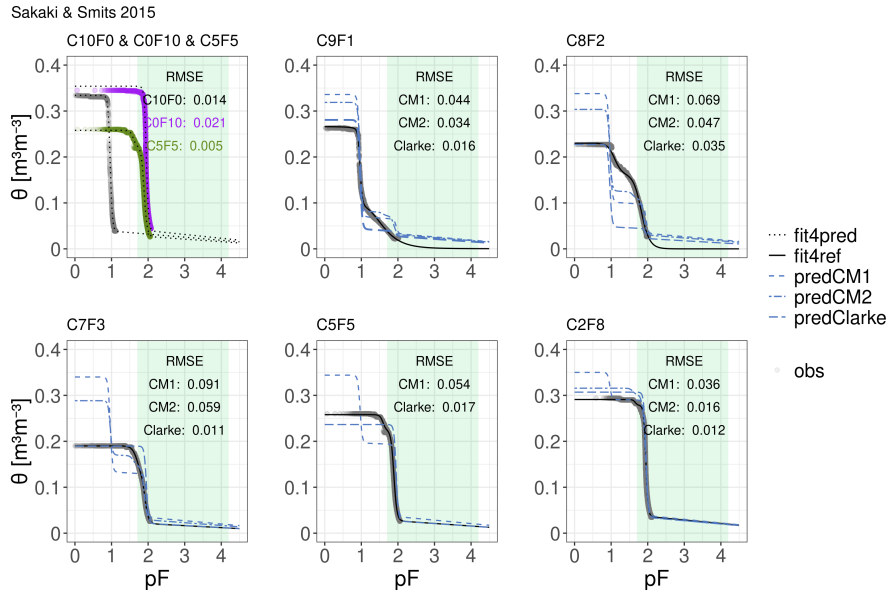
Figure 4. Water retention curves of all seven binary mixtures produced from coarse sand (C10F0) and fine sand (C0F10). Observations („obs") are represented by gray dots, fitted curves are represented by black lines (i.e reference curves as solid lines, „fit4ref", see Tab. A2 for fitting parameters and model specification). The predicted curves („pred") are represented by blue dashed lines. CM1 stands for the basic compositional model and CM2 for the extended scheme, Clarke stands for the adapted model from Clarke (1979). The first panel (top, left) assembles the fitted water retention curves of the pure components and the intermediate mixture as dotted black lines („fit4pred"), which constitute the input for the compositional model. The particular RMSE describes the deviation between the predictions and the reference curves. Note that C5F5 is not predicted by the extended model scheme because it is considered the intermediate mixture.

reference WRC is generally smaller than 2 %. Using the extended scheme improves the prediction regarding the RMSE in three of four cases (mixture C4B6, C3B7 and C2B8). The compositional model led to similarly good results for the data of

280 Walczak et al. (2002) (Fig. 6). Here the RMSE between the predicted curves and reference curves ranges from $0.01\,\mathrm{m^3\,m^{-3}}$ to $0.03\,\mathrm{m^3\,m^{-3}}$, having the same order of magnitude as the errors calculated between the observations and corresponding fitted curves, ranging from $0.006\,\mathrm{m^3\,m^{-3}}$ to $0.029\,\mathrm{m^3\,m^{-3}}$ (Tab. A4). Using the extended scheme for this data set improves the representation in the average for the mixtures P2S8, P8S2, P9S1. The improvements using CM2 are especially observable for pF-values above 1.2. The deviations here reflect the comparably poor fit of the original unimodal constrained model of van

285 Genuchten (1980) used to mathematically represent the data of the pure peat (RMSE $0.029\,\mathrm{m^3\,m^{-3}}$). This leads to deviations in the predictions which remain smaller if the extended scheme is applied.
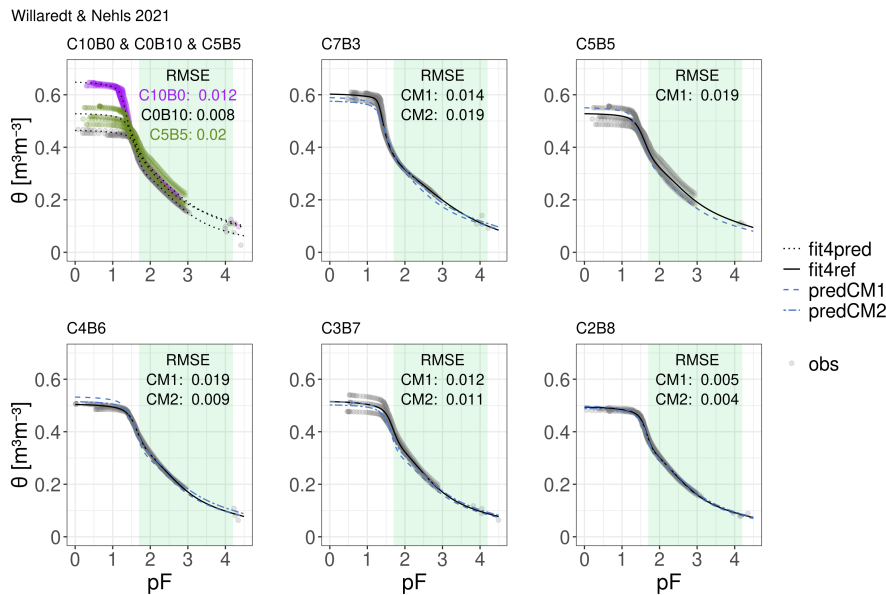
Figure 5. Water retention curves of all seven binary mixtures of ground bricks (C0B10) and green waste compost (C10B0). Observations ("obs") are represented by gray dots, fitted curves are represented by black lines (i.e reference curves as solid lines, "fit4ref", see Tab. A1 for fitting parameters and model specification). The predicted curves ("pred") are represented by blue dashed lines. CM1 stands for the basic compositional model and CM2 for the extended scheme. The first panel (top, left) assembles the fitted water retention curves of the pure components and the intermediate mixture as dotted black lines ("fit4pred"), which constitute the input for the compositional model. The particular RMSE describes the deviation between the predictions and the reference curves. Note that C5B5 is not predicted by the extended model scheme because it is considered the intermediate mixture.

3.4 Absolute deviations along the water retention curve

The RMSE, as a measure averaging deviations between predicted and reference curves, can mask the mal performance of the predictions in some parts of the curve. Therefore, considering the absolute deviations (compare Fig. 8) over different matric potentials completes the assessment. Generally, for the data set of Willaredt and Nehls (2021), the deviation over all matric potentials does not exceed 4.2 % and is largest in the wet range. That is not surprising, since the retention characteristics close to saturation are highly influenced by soil structure and thus hardly predictable. The predictions made using the basic compositional model approach (CM1) tend to overestimate the water contents. Compared to that, the extended scheme underestimates the water contents in the same pressure head range. Applying the extended scheme diminishes the absolute deviation only for the mixture C4B6, which has mixing ratio close to the intermediate mixture. For the data set of Walczak et al. (2002) using the extended scheme CM2 yields more accurate predictions in the dry range for mixtures containing volumetric shares of peat $x_v > 0.6$.
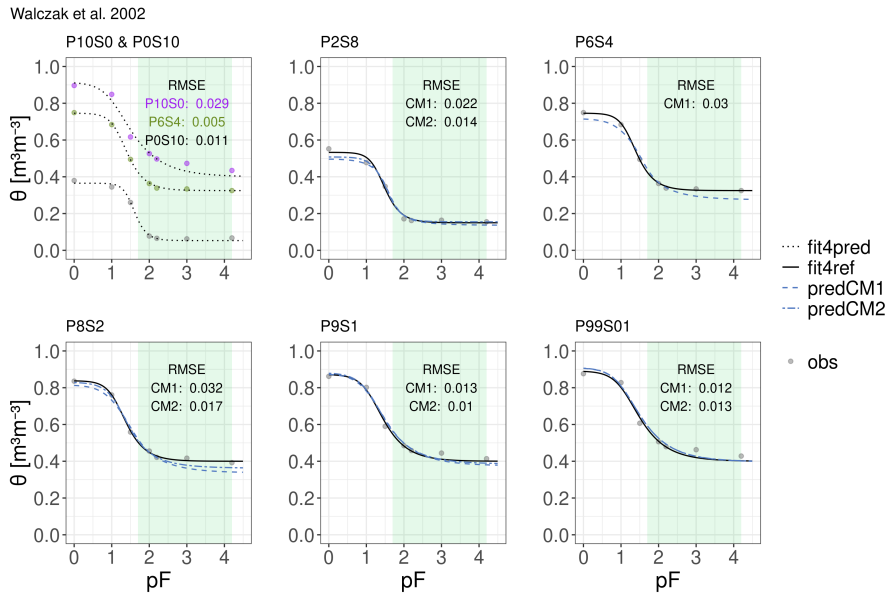
Figure 6. Retention curves of all seven binary mixtures of sand (P0S10) and peat (P10S0). Observations („obs") are represented by gray dots, fitted curves are represented by black lines (i.e reference curves as solid lines, „fit4ref", see Tab. A4 for fitting parameters and model specification). The predicted curves („pred") are represented by blue dashed lines. CM1 stands for the basic compositional model and CM2 for the extended scheme. The first panel (top, left) assembles the fitted water retention curves of the pure components and the intermediate mixture as dotted black lines („fit4pred"), which constitute the input for the compositional model. The particular RMSE describes the deviation between the predictions and the reference curves. Note that P6S4 is not predicted by the extended model scheme because it is considered the intermediate mixture.

Obviously, the method used for determining the water retention curves of the main components has an impact on the prediction quality. The case of a larger deviation of the observed water contents between replicates leads to poor representations by the parametric fits that are used to predict water retention curves of other mixtures. On the one hand, the deviation between the replicates of the components introduces an error when being used as model input for predicting the WRC of the mixtures. On the other hand, the deviation resulting from the uncertainties of sample preparation of any mixture also defines the magnitude of the tolerable error when predicting the curves by the means of our model approach. The tested data sets of Deeb et al. (2016) and Willaredt and Nehls (2021) were derived from replicated observations (compare Fig. 7 and 5). In addition to the RMSEs summarised in the corresponding figures, Tab. 3 provides the absolute maximal and minimal deviations from the corresponding mathematical representation for each observed mixture in the data set of Deeb et al. (2016) and Willaredt and Nehls (2021), thus providing the magnitude of the tolerable error by our predictions. Those deviations are bigger for the data set obtained by Deeb et al. (2016) using a more practice-oriented sampling strategy from containers. Along the observed pressure head
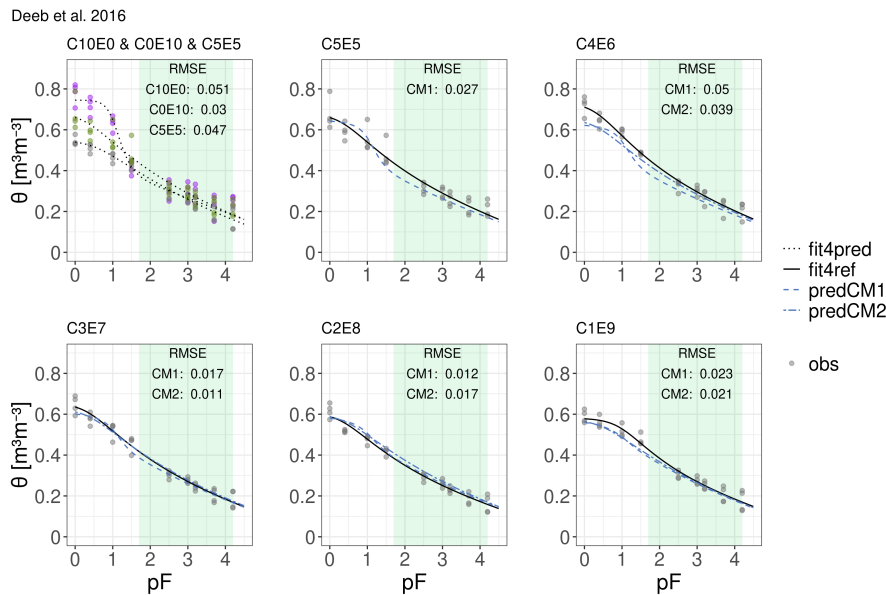
Figure 7. Water retention curves of all 7 binary mixtures of excavated deep soil horizon (C0E10) and green waste compost (C10E0). Observations („obs") are represented by gray dots, fitted curves are represented by black lines (i.e reference curves as solid lines, „fit4ref", see Tab. A3 for fitting parameters and model specification). The predicted curves („pred") are represented by blue dashed lines. CM1 stands for the basic compositional model and CM2 for the extended scheme. The first panel (top, left) assembles the fitted water retention curves of the pure components and the intermediate mixture as dotted black lines („fit4pred"), which constitute the input for the compositional model. The particular RMSE describes the deviation between the predictions and the reference curves. Note that C5E5 is not predicted by the extended model scheme because it is considered the intermediate mixture.

range the biggest deviations occur in the mixture C5E5. Here the parametric fit underestimated the observed water contents in the worst case by 13 %. The deviations remain similarly large along all observed matric potentials. Following the sampling preparation protocol introduced by Willaredt and Nehls (2021) yields comparably smaller deviations of bulk densities. Here the biggest misfit for the WRCs was observed for the mixture C7B3, where the parametric representation underestimates the observation by 5 %. In Fig. 8 it can be observed that the deviations decrease for higher tensions, except for the mixture C5B5. According to Jackisch et al. (2020), this reflects a deviation related to different bulk densities of samples that are homogeneous otherwise. However, the deviations related to different compaction of Technosols when used in practice are expected to be larger. Figure 8 visualizes the absolute deviations between the predictions and the parametric representations for all predicted WRC. In the data sets from Willaredt and Nehls (2021) as well as from Deeb et al. (2016) the deviations remain smaller than the maximum deviations described in the section above.
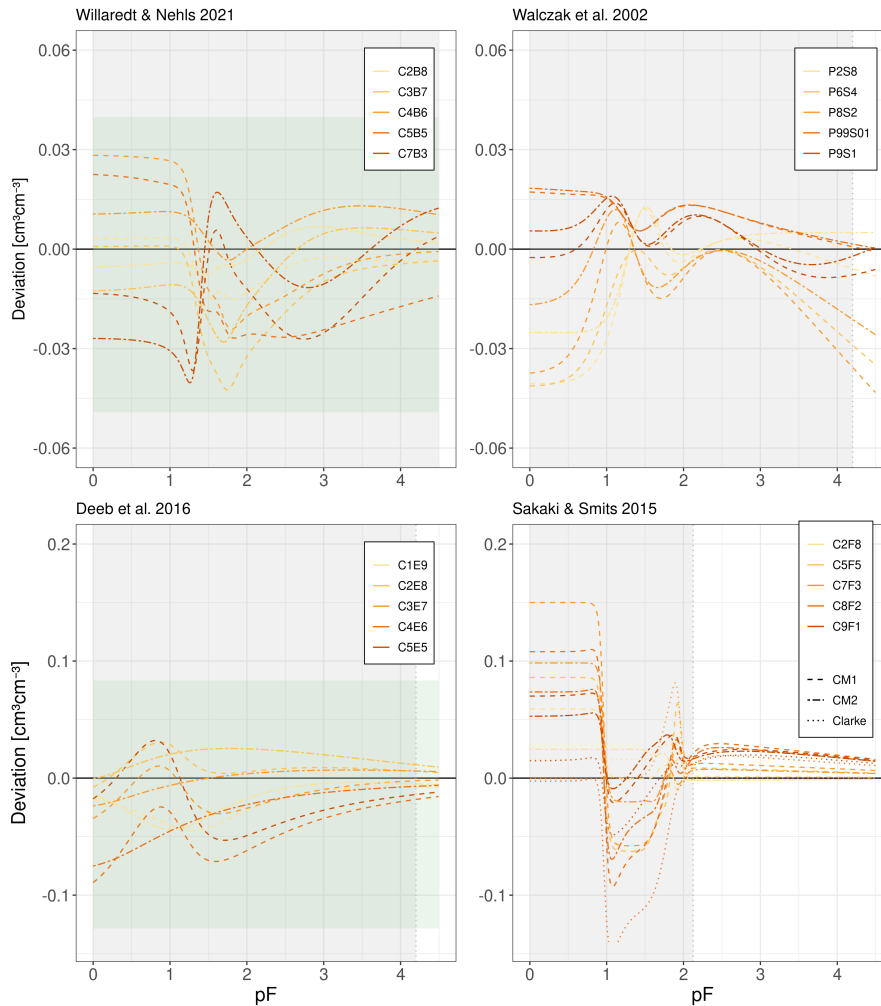
Figure 8. Absolute deviation between predicted and reference water contents over different matric potentials. The shaded pressure head range in gray was covered by measurements. The solid line represents the deviation between predictions with the basic model scheme (CM1) and the reference values. The dashed line represents the deviation between the extended model scheme (CM2) and the reference values. The green ribbon illustrates the maximum deviation that occurred between the observations and fitted mathematical representations.

3.5 Comparison of basic and extended scheme

320 The plots in Fig. 8 show that, for the CM1 model, the largest deviations occur in the wet range, with the exception of the data set of Walczak et al. (2002). The extended scheme CM2 leads to smaller RMSE and also to smaller absolute deviations, except for a few cases: in the wet range for the mixture C7B3 of the data set by Willaredt and Nehls (2021) and in the medium to dry range for the mixture C2E8 of the data set by Deeb et al. (2016). Nonetheless, the curves predicted using the basic compositional model approach already represent the observations with a quality that does not warrant further improvement by

Table 3. Maximum and minimum deviation between observations and the corresponding mathematical representations of volumetric water contents of all observed matric potentials. The magnitude reflects the differences between the replicates due to different sampling strategies (packing cylinders to a defined weight for compaction vs. in situ sampling from containers).

| | Willaredt & Nehls 2021 | | | Deeb et al. 2016 | |
Mixture	Min deviation $[\mathrm{m^3\,m^{-3}}]$	Max deviation $[\mathrm{m^3\,m^{-3}}]$	Mixture	Min deviation $[\mathrm{m^3\,m^{-3}}]$	Max deviation $[\mathrm{m^3\,m^{-3}}]$
C0B10	-0.04	0.04	C0E10	-0.06	0.05
C2B8	-0.01	0.01	C1E9	-0.06	0.04
C3B7	-0.03	0.04	C2E8	-0.07	0.05
C4B6	-0.02	0.02	C3E7	-0.05	0.06
C5B5	-0.04	0.04	C4E6	-0.05	0.07
C7B3	-0.05	0.02	C5E5	-0.13	0.08
C10B0	-0.04	0.02	C10E0	-0.09	0.08

325 additional laboratory work. However, an additional measurement of an intermediate mixture can always serve as a validation measurement, demonstrating that the approach does not fail for the chosen components of the Technosol formulation.

3.6 Model application for constructed Technosols

Based on the predicted water retention curves, it is possible to analyse and compare the hydrologic performance of constructed Technosols, e.g. as planting substrates in urban green infrastructure. We can analyse the behaviour and perform the comparisons

330 of: i) any possible mixing ratio, and ii) different components. The first type of comparison narrows down the infinite options provided by combining two components to a full range of mixtures. The second type of comparison enables exploration of the behaviour of potential components in mixtures and selection of the most suitable components, that provide plant growth supporting properties.

3.6.1 Hydraulic conductivity prediction

335 Figure 9 and Tab. 4 show the predicted hydraulic conductivity curves and the so-called saturated matrix conductivity ($K_{s,matrix}$). As expected for the wet range, the conductivity is higher in the coarser green waste compost, with $390\,\mathrm{cm\,d^{-1}}$ compared to the conductivity in ground bricks with $61\,\mathrm{cm\,d^{-1}}$ at a matric potential corresponding to pF 0.8 in the mixtures formulated by Willaredt and Nehls (2021). For the data set of Deeb et al. (2016), the conductivity spans a similar range with $670\,\mathrm{cm\,d^{-1}}$ in green waste compost and $47\,\mathrm{cm\,d^{-1}}$ in excavated deep soil.

340 The compositional model approach to predict the WRCs, together with the scheme for predicting the unsaturated hydraulic conductivity for the full range of pressure heads by Peters et al. (2023, 2021), allows full characterisation of the soil hydraulic properties of any binary mixture. The properties required for modelling transient flow and transport processes in urban green

Table 4. Predicted saturated matrix conductivity for all mixtures of the full mixing range. $K_{s,matrix}$ mimics the saturated conductivity for the case if macro pores are present (Peters et al., 2023)

Willaredt & Nehls 2021		Deeb et al. 2016	
Mixture	K_s [$\mathrm{cm\,d^{-1}}$]	Mixture	K_s [$\mathrm{cm\,d^{-1}}$]
C0B10	61	C0E10	46
C2B8	100	C1E9	48
C3B7	130	C2E8	63
C4B6	160	C3E7	93
C5B5	200	C4E6	140
C7B3	260	C5E5	200
C10B0	390	C10E0	670

infrastructure elements, as demonstrated in Brunetti et al. (2016), can thus be obtained solely based on the measured water retention characteristics of the pure components that constitute the mixture. These results enable the design of Technosol compositions, as well as container dimensions of urban green infrastructure dedicated for water management applications under realistic atmospheric boundary conditions.

3.6.2 A case study of predicted water and air distribution

For a hydrostatic case, we calculated the distribution of water and air contents in binary mixtures of Willaredt and Nehls (2021) and Deeb et al. (2016). Here, we assume that the Technosols are implemented as planting substrates in a container of $0.5\,\mathrm{m}$ depth. Figure 10 shows the vertical distribution of water and air under such conditions. A volumetric air content of at least 15 % throughout the depth is a favourable condition for root growth (Caron et al., 2015). We conclude for both Technosols that green waste compost introduces the pore space to the mixture that is needed to guarantee supply of air for the roots in shallow containers. For Technosols that contain ground bricks as a mineral component, the GWC content has to be at least 70 vol% to omit insufficient air supply in shallow containers. Alternatively, the depth of containers should be increased for mixtures containing less GWC. Technosols formulated with excavated deep soil present sufficient supply of air in shallow containers when containing at least 20 vol% GWC, this confirms the results in Deeb et al. (2016).

4 Conclusions

This study presents a compositional model that allows us to predict the water retention curve (WRC) of a constructed Technosol formulated as a binary mixture of any mixing ratio. The predictions are based on the measured WRC of the pure components and the volumetric mixing ratio. Thus, only a small measurement effort is required for describing a large number of possible combinations. The introduced compositional model approach, in the basic as well as extended scheme, was shown to be ap-
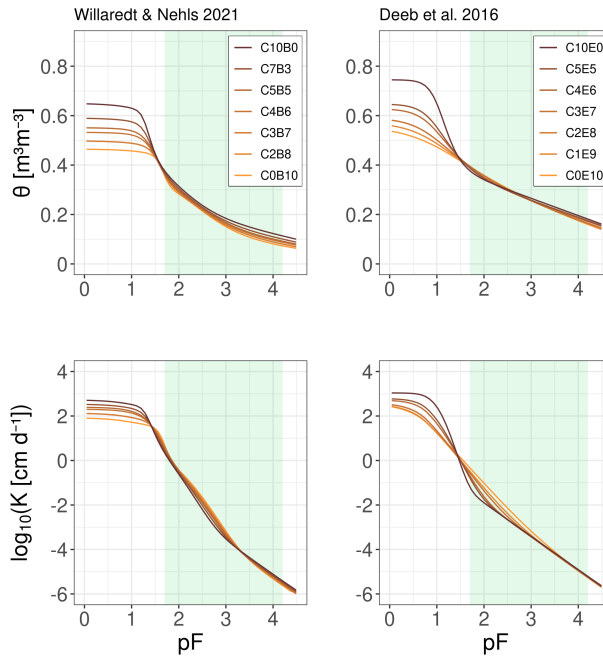
Figure 9. Predicted soil hydraulic properties of binary mixtures. In the left column mixtures are formulated from green waste compost and ground bricks and in the right column from green waste compost and excavated deep soil. WRCs were predicted using the compositional model in the simple scheme (CM1) and the soil hydraulic conductivity was predicted using the the approaches of Peters et al. (2021, 2023).

plicable to mixtures of components characterised by a small difference in their pore space distribution maxima (ΔPSD_{max}). It can be concluded that the model performs best based on water retention observations that have a high reproducibility, a high resolution and which cover a large range of pressure heads. From the comparison between predicted and reference WRCs of three case study mixtures that are of practical relevance for Technosol construction, we conclude that the approach should be valid for further materials and their compositions. In order to demonstrate practical applications of the predicted WRCs, the unsaturated hydraulic conductivity as well as the hydrostatic distribution of water and air in constructed Technosols was predicted. The knowledge of the soil hydraulic properties of any mixing ratio enables the quick choice of a binary Technosol composition, based on either estimated air capacity, wilting point capacity and available water capacity or the modelled water balance of a soil-plant-atmosphere system e.g. in urban green infrastructure. Through this, planning for efficient water management in urban green infrastructure dedicated to different purposes (e.g. rainwater, grey water, irrigation etc.), is made possible. The results of this study indicate the added value of a systematic soil hydrological characterisation of potential Technosol components e.g. in the form a database. Such data could be used to further evaluate the compositional model approach and for theoretical experiments which search for purpose-designed Technosol recipes.
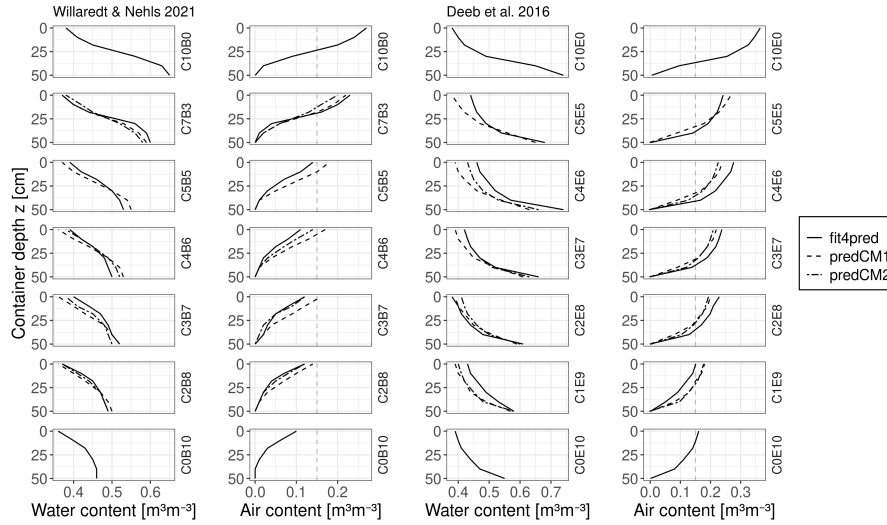
Figure 10. Distribution of volumetric water and air content over different depths at hydrostatic equilibrium in a container (corresponding to pF = 1.7 at the top of the container) filled with a constructed Technosol formulated as a binary mixture of: green waste compost and ground bricks (left) and green waste compost and excavated deep soil (right). The solid line indicates the reference WRCs, the dashed lines indicate predictions using the basic scheme (CM1) or the extended scheme (CM2) respectively. The grey vertical line indicates the minimum volumetric air content in horticultural substrates favourable for root growth (Caron et al., 2015).

375 *Data availability.* In the appendix we provide the fitting parameters and WRC models used to represent the water retention data sets presented in this study. The raw data from third parties can not be made available. The raw data related to the work by Willaredt and Nehls (2021) can be obtained upon request from the corresponding author.

Appendix A: Description of water retention models used for mathematical representation

The data of Willaredt and Nehls (2021) was represented with the PDI (Peters, 2013; Iden and Durner, 2014; Peters, 2014)
380 model with the unconstrained bimodal (Durner, 1994) basic function of van Genuchten (1980), the respective parameters are displayed in Tab. A1. The PDI model accounts for both capillary and adsorptive water retention (S^{cap} [-] and S^{ad} [-]) :

$$\theta(h) = (\theta_s - \theta_r) \cdot S^{cap} + \theta_r S^{ad}. \tag{A1}$$

where $\theta(h)$ [m^3 m^{-3}] stands for the volumetric water content and h [cm] stands for the matric potential. To ensure that the water content is 0 for $h = h_0 = 10^{6.8}$ [cm], the respective basic function in the capillary saturation function $\Gamma(h)$ is scaled as follows:

$$S^{cap}(h) = \frac{\Gamma(h) - \Gamma_0}{1 - \Gamma_0} \tag{A2}$$

with $\Gamma_0 = \Gamma(h_0)$. The basic function $\Gamma(h)$ in form of the constrained retention function of van Genuchten (1980) is described by:

$$\Gamma(h) = \left[\frac{1}{1+(\alpha h)^n}\right]^{1-\frac{1}{n}}. \tag{A3}$$

where α [cm^{-1}] and n [-] are curve shape parameters. The unconstrained function of van Genuchten (1980) is described by:

$$\Gamma(h) = \left[\frac{1}{1+(\alpha h)^n}\right]^{m}. \tag{A4}$$

where m [-] stands for an additional shape parameter. In the bimodal form of (Durner, 1994) the basic functions are weighted and added:

$$\Gamma(h) = \sum_{i=1}^{2} w_i \Gamma_i \tag{A5}$$

with w_i standing for the weighting factor of the sub functions, with $0 < w_i < 1$ and $\sum w_i = 1$. The adsorptive water retention is calculated as:

$$S^{ad}(x) = 1 + \frac{1}{x_a - x_0}\left(x - x_a + b\, ln\left[1 + \exp\left(\frac{x_a - x}{b}\right)\right]\right) \tag{A6}$$

where x is standing for $x = pF = \log_{10}(h)$, with h in [cm^{-1}]. Here x_a refers to the pF value corresponding to the suction at air entry for adsorptive retention, with $x_a = pF = \log_{10}(h_a)$ and x_0 refers to the pF value corresponding to the suction, where the water content is zero: $x_0 = pF = \log_{10}(h_0)$. The smoothing parameter b for the adsorption function in the constrained and unconstrained van Genuchten function is calculated with:

$$b = 0.1 + \frac{0.2}{n^2}\left[1 - \exp\left(-\frac{\theta_r}{\theta_s - \theta_r}\right)\right]^2 \tag{A7}$$

Table A1. Fitted Parameters to water retention observations from Willaredt & Nehls 2021, bimodal PDI unconstrained van Genuchten variant and RMSE between model and observations.

Mixture	$x_{i,v}$ [$m^3\,m^{-3}$]	α_1 [cm^{-1}]	n_1 [-]	θ_r [$m^3\,m^{-3}$]	θ_s [$m^3\,m^{-3}$]	α_2 [cm^{-1}]	n_2 [-]	w_2 [-]	m_1 [-]	m_2 [-]	RMSE [$m^3\,m^{-3}$]
C0B10	0	0.00335	0.933	0.134	0.465	0.0213	5.902	0.361	1 *	1 *	0.008
C2B8	0.18	0.00448	0.963	0.159	0.495	0.0224	5.204	0.342	1 *	1 *	0.006
C3B7	0.28	0.00442	0.952	0.166	0.516	0.0211	4.462	0.314	0.999	1 *	0.015
C4B6	0.37	0.00404	0.932	0.168	0.505	0.0231	3.856	0.347	1 *	1 *	0.005
C5B5	0.47	0.00413	0.926	0.209	0.529	0.0257	3.468	0.433	1 *	1 *	0.02
C7B3	0.68	0.0054	0.824	0.148	0.604	0.0473	9.382	0.495	0.531	0.228	0.014
C10B0	1 *	0.00935	0.968	0.237	0.65	0.0514	6.879	0.515	1 *	0.346	0.012

* Parameter boundary reached

Table A2. Fitted Parameters to water retention observations from Sakaki and Smits (2015), bimodal PDI constrained van Genuchten variant

Mixture	$x_{i,v}$ [$m^3\,m^{-3}$]	α_1 [cm^{-1}]	n_1 [-]	θ_r [$m^3\,m^{-3}$]	θ_s [$m^3\,m^{-3}$]	α_2 [cm^{-1}]	n_2 [-]	w_2 [-]	RMSE [$m^3\,m^{-3}$]
C0F10	0	0.0112	15 *	0.04	0.354	0.00143	8.701	0 *	0.021
C2F8	0.2	0.0113	15 *	0.039	0.291	0.0221	14.057	0.046	0.009
C5F5	0.7	0.013	11.104	0.029	0.258	0.0258	10.319	0.148	0.005
C7F3	0.7	0.0123	9.857	0.022	0.19	0.0199	5.937	0.429	0.002
C8F2	0.8	0.0852	4.698	0 *	0.23	0.0162	4.341	0.699	0.004
C9F1	0.9	0.1089	15 *	0.001	0.266	0.043	2.171	0.388	0.005
C10F0	1	0.1092	15 *	0.039	0.334	0.00049	1.02	0 *	0.014

* Parameter boundary reached

A1 Fitting parameters

In the following the fitting parameters obtained for every mixture of each data set are presented in Tab. A1-A4 with the corresponding RMSE as a diagnostic variable describing the mean deviation between the fitted model and the observation. The data set of Sakaki and Smits (2015) was described with the PDI model using the constrained bimodal van Genuchten function (Durner, 1994). The respective parameters are displayed in Tab. A2.

The data set of Deeb et al. (2016) was represented using the PDI model with the unimodal constrained van Genuchten function as basic function, the respective parameters are displayed in Tab. A3.

The data set of Walczak et al. (2002) was represented using the original unimodal constrained model of van Genuchten (1980), the respective parameters are displayed in Tab. A4.

Table A3. Fitted Parameters to water retention observations from Deeb et al. (2016), unimodal PDI constrained van Genuchten variant

Mixture	$x_{i,v}$ $[\mathrm{m^3\,m^{-3}}]$	α $[\mathrm{cm^{-1}}]$	n $[-]$	θ_r $[\mathrm{m^3\,m^{-3}}]$	θ_s $[\mathrm{m^3\,m^{-3}}]$	RMSE $[\mathrm{m^3\,m^{-3}}]$
C0E10	0	0.31	1.109	0.161	0.551	0.03
C1E9	0.1	0.1144	1.336	0.345	0.581	0.029
C2E8	0.2	0.5 *	1.235	0.33	0.609	0.028
C3E7	0.3	0.5 *	1.208	0.326	0.658	0.031
C4E6	0.4	0.5 *	1.258	0.4 *	0.737	0.032
C5E5	0.5	0.5 *	1.245	0.4 *	0.682	0.047
C10E0	1	0.0843	2.949	0.4 *	0.745	0.05

* Parameter boundary reached

Table A4. Fitted Parameters to water retention observations from Walczak et al. (2002), original unimodal constrained van Genuchten model

Mixture	$x_{i,v}$ $[\mathrm{m^3\,m^{-3}}]$	α $[\mathrm{cm^{-1}}]$	n $[-]$	θ_r $[\mathrm{m^3\,m^{-3}}]$	θ_s $[\mathrm{m^3\,m^{-3}}]$	RMSE $[\mathrm{m^3\,m^{-3}}]$
P0S10	0	0.0295	3.148	0.053	0.365	0.011
P2S8	0.24	0.0447	2.482	0.15	0.533	0.017
P6S4	0.64	0.058	2.307	0.325	0.746	0.006
P8S2	0.82	0.0682	2.144	0.4 *	0.838	0.008
P9S1	0.93	0.071	1.74	0.4 *	0.872	0.017
P99S01	0.99	0.0753	1.881	0.4 *	0.891	0.025
P10S0	1	0.0839	1.641	0.4 *	0.914	0.029

* Parameter boundary reached

Author contributions. Conceptualization, M.W. and T.N.; Model implementation and Analysis, M.W., A.P. and T.N. writing - original draft preparation, M.W; writing - review and editing, M.W., T.N., A.P. ; All authors read and approved the final manuscript.

Competing interests. The authors declare that there are no competing interests.

415 *Acknowledgements.* We would like to thank Maha Deeb, Toshihiro Sakaki and Kathleen M. Smits for providing water retention data. M. Willaredt thanks the Berlin International Graduate School on Model and Simulation Based Research (BIMoS) for funding her dissertation project. T. Nehls thanks the BMWi (Ugreen, FKZ 03EN1045C). A.Peters thanks the DFG (Deutsche Forschungsgemeinschaft (DFG grant

PE 1912/4-1)). We thank Sarah Sanford and Anna Rowntree for linguistic revision. Further, we thank two anonymous reviewers for their comments and feedback, which have contributed to improve our manuscript.

References

Abel, S., Peters, A., Trinks, S., Schonsky, H., Facklam, M., and Wessolek, G.: Impact of biochar and hydrochar addition on water retention and water repellency of sandy soil, Geoderma, 202, 183–191, 2013.

Al Naddaf, O., Livieratos, I., Stamatakis, A., Tsirogiannis, I., Gizas, G., and Savvas, D.: Hydraulic characteristics of composted pig manure, perlite, and mixtures of them, and their impact on cucumber grown on bags, Scientia horticulturae, 129, 135–141, 2011.

Bouwer, H. and Rice, R.: Hydraulic Properties of Stony Vadose Zones a, Groundwater, 22, 696–705, 1984.

Brunetti, G., Šimůnek, J., and Piro, P.: A comprehensive analysis of the variably saturated hydraulic behavior of a green roof in a mediterranean climate, Vadose Zone Journal, 15, 2016.

Campbell, G. S., Smith, D. M., and Teare, B. L.: Application of a dew point method to obtain the soil water characteristic, in: Experimental unsaturated soil mechanics, pp. 71–77, Springer, 2007.

Caron, J., Price, J., and Rochefort, L.: Physical properties of organic soil: adapting mineral soil concepts to horticultural growing media and histosol characterization, Vadose Zone Journal, 14, 2015.

Clarke, R.: Reservoir properties of conglomerates and conglomeratic sandstones: Geologic notes, AAPG bulletin, 63, 799–803, 1979.

Deeb, M., Grimaldi, M., Lerch, T. Z., Pando, A., Podwojewski, P., and Blouin, M.: Influence of organic matter content on hydro-structural properties of constructed Technosols, Pedosphere, 26, 486–498, 2016.

Deeb, M., Groffman, P. M., Blouin, M., Egendorf, S. P., Vergnes, A., Vasenev, V., Cao, D. L., Walsh, D., Morin, T., and Séré, G.: Using constructed soils for green infrastructure – challenges and limitations, SOIL, 6, 413–434, https://doi.org/10.5194/soil-6-413-2020, 2020.

Durner, W.: Hydraulic conductivity estimation for soils with heterogeneous pore structure, Water resources research, 30, 211–223, 1994.

Eksi, M., Sevgi, O., Akburak, S., Yurtseven, H., and Esin, İ.: Assessment of recycled or locally available materials as green roof substrates, Ecological Engineering, 156, 105 966, 2020.

Fabbri, D., Pizzol, R., Calza, P., Malandrino, M., Gaggero, E., Padoan, E., and Ajmone-Marsan, F.: Constructed Technosols: A Strategy toward a Circular Economy, Applied Sciences, 11, 3432, https://doi.org/https://doi.org/10.3390/app11083432, 2021.

Fields, J. S., Owen, J. S., Altland, J. E., van Iersel, M. W., and Jackson, B. E.: Soilless substrate hydrology can be engineered to influence plant water status for an ornamental containerized crop grown within optimal water potentials, Journal of the American Society for Horticultural Science, 143, 268–281, 2018.

Flint, A. L. and Childs, S.: Physical properties of rock fragments and their effect on available water in skeletal soils, Erosion and productivity of soils containing rock fragments, 13, 91–103, 1984.

Flores-Ramírez, E., Abel, S., and Nehls, T.: Water retention characteristics of coarse porous materials to construct purpose-designed plant growing media, Soil science and plant nutrition, 64, 181–189, 2018.

Grabowski, Z. J., McPhearson, T., Matsler, A. M., Groffman, P., and Pickett, S. T.: What is green infrastructure? A study of definitions in US city planning, Frontiers in Ecology and the Environment, 2022.

Hill, J., Sleep, B., Drake, J., and Fryer, M.: The Effect of Intraparticle Porosity and Interparticle Voids on the Hydraulic Properties of Soilless Media, Vadose Zone Journal, 18, 2019.

Iden, S. C. and Durner, W.: Comment on "Simple consistent models for water retention and hydraulic conductivity in the complete moisture range" by A. Peters, Water Resources Research, 50, 7530–7534, 2014.

Jackisch, C., Germer, K., Graeff, T., Andrä, I., Schulz, K., Schiedung, M., Haller-Jans, J., Schneider, J., Jaquemotte, J., Helmer, P., et al.: Soil moisture and matric potential–an open field comparison of sensor systems, Earth System Science Data, 12, 683–697, 2020.

Mark Mitchell, B. M. and et al, T. W.: Engauge Digitizer Software, online, http://markummitchell.github.io/engauge-digitizer, 2019.

Molineux, C. J., Fentiman, C. H., and Gange, A. C.: Characterising alternative recycled waste materials for use as green roof growing media in the UK, Ecological Engineering, 35, 1507–1513, 2009.

460   Naseri, M., Iden, S. C., Richter, N., and Durner, W.: Influence of stone content on soil hydraulic properties: experimental investigation and test of existing model concepts, Vadose Zone Journal, 18, 2019.

Nehls, T., Rokia, S., Mekiffer, B., Schwartz, C., and Wessolek, G.: Contribution of bricks to urban soil properties, Journal of soils and sediments, 13, 575–584, 2013.

Nehls, T., Schwartz, C., Kim, K.-H. J., Kaupenjohann, M., Wessolek, G., and Morel, J.-L.: Letter to the editors: Phyto-P-mining, secondary
465   urban green recycles phosphorus from soils constructed of urban wastes, Journal of soils and sediments, 15, 1667–1674, 2015.

Peters, A.: Simple consistent models for water retention and hydraulic conductivity in the complete moisture range, Water Resources Research, 49, 6765–6780, 2013.

Peters, A.: Reply to comment by S. Iden and W. Durner on "Simple consistent models for water retention and hydraulic conductivity in the complete moisture range", Water Resources Research, 50, 7535–7539, 2014.

470   Peters, A. and Durner, W.: SHYPFIT 2.0 Users Manual. Research Report, Institut für Ökologie, Technische Universität Berlin, Germany., 2015.

Peters, A., Iden, S. C., and Durner, W.: Revisiting the simplified evaporation method: Identification of hydraulic functions considering vapor, film and corner flow, Journal of hydrology, 527, 531–542, 2015.

Peters, A., Hohenbrink, T. L., Iden, S. C., and Durner, W.: A simple model to predict hydraulic conductivity in medium to dry soil from the
475   water retention curve, Water Resources Research, 57, e2020WR029 211, 2021.

Peters, A., Hohenbrink, T. L., Iden, S. C., van Genuchten, M. T., and Durner, W.: Prediction of the absolute hydraulic conductivity function from soil water retention data, Hydrology and Earth System Sciences Discussions. Preprint., pp. 1–32, https://doi.org/10.5194/hess-2022-431, 2023.

Pitton, B. J., Oki, L. R., Sisneroz, J., and Evans, R. Y.: A nursery system nitrogen balance for production of a containerized woody ornamental
480   plant, Scientia Horticulturae, 291, 110 569, 2022.

Pouyat, R. V., Szlavecz, K., Yesilonis, I. D., Groffman, P. M., and Schwarz, K.: Chemical, physical and biological characteristics of urban soils. Chapter 7, vol. 55 of *Agronomy Monograph*, chap. 7, pp. 119–152, 2010.

Prado, B., Mora, L., Abbruzzini, T., Flores, S., Cram, S., Ortega, P., Navarrete, A., and Siebe, C.: Feasibility of urban waste for constructing Technosols for plant growth, Revista Mexicana de Ciencias Geológicas, 37, 237–249, 2020.

485   Rokia, S., Séré, G., Schwartz, C., Deeb, M., Fournier, F., Nehls, T., Damas, O., and Vidal-Beaudet, L.: Modelling agronomic properties of Technosols constructed with urban wastes, Waste management, 34, 2155–2162, 2014.

Sakaki, T. and Illangasekare, T. H.: Comparison of height-averaged and point-measured capillary pressure–saturation relations for sands using a modified Tempe cell, Water resources research, 43, 2007.

Sakaki, T. and Smits, K. M.: Water Retention Characteristics and Pore Structure of Binary Mixtures, Vadose Zone Journal, 14,
490   https://doi.org/10.2136/vzj2014.06.0065, 2015.

Schindler, U.: Ein Schnellverfahren zur Messung der Wasserleitfähigkeit im teilgesättigten Boden and Stechzylinderproben, Archiv fur Acker-und Pflanzenbau und Bodenkunde, 1980.

Tams, L., Nehls, T., and Calheiros, C. S. C.: Rethinking green roofs-natural and recycled materials improve their carbon footprint, Building and Environment, 219, 109 122, 2022.

495 Ulrich, S., Willaredt, M., Nehls, T., and van Schaik, L.: Do earthworms (D. veneta) influence plant-available water in technogenic soil-like substrate from bricks and compost?, Journal of Soils and Sediments, 21, 2013–2024, 2021.

van Genuchten, M. T.: A closed-form equation for predicting the hydraulic conductivity of unsaturated soils, Soil science society of America Journal, 44, 892–898, 1980.

Vidal-Beaudet, L., Rokia, S., Nehls, T., and Schwartz, C.: Aggregation and availability of phosphorus in a Technosol constructed from urban
500 wastes, Journal of soils and sediments, 18, 456–466, 2018.

Walczak, R., Rovdan, E., and Witkowska-Walczak, B.: Water retention characteristics of peat and sand mixtures, International Agrophysics, 16, 2002.

Willaredt, M. and Nehls, T.: Investigation of water retention functions of artificial soil-like substrates for a range of mixing ratios of two components, Journal of Soils and Sediments, 21, 2118–2129, 2021.

505 Yilmaz, D., Cannavo, P., Séré, G., Vidal-Beaudet, L., Legret, M., Damas, O., and Peyneau, P.-E.: Physical properties of structural soils containing waste materials to achieve urban greening, Journal of soils and sediments, 18, 442–455, 2018.

Zhang, Z. F., Ward, A. L., and Keller, J. m.: Determining the porosity and saturated hydraulic conductivity of binary mixtures, Vadose Zone Journal, 10, 313–321, 2011.